OXFORD
SOT | Society of Toxicology
www.toxsci.oxfordjournals.org

TOXICOLOGICAL SCIENCES, 150(1), 2016, 204–215

doi: 10.1093/toxsci/kfv319
Advance Access Publication Date: December 31, 2015
Research Article

Low Dose Acetaminophen Induces Reversible Mitochondrial Dysfunction Associated with Transient c-Jun N-Terminal Kinase Activation in Mouse Liver

Jiangting Hu,[*,†] Venkat K. Ramshesh,[*,†,‡] Mitchell R. McGill,[§] Hartmut Jaeschke,[§] and John J. Lemasters[*,†,‡,¶,1]

[*]Center for Cell Death, Injury & Regeneration; [†]Departments of Drug Discovery & Biomedical Sciences and Biochemistry & Molecular Biology; [‡]Hollings Cancer Center, Medical University of South Carolina, Charleston, South Carolina 29425; [§]Department of Pharmacology, Toxicology & Therapeutics, University of Kansas Medical Center, Kansas City, Kansas 66160; and [¶]Institute of Theoretical & Experimental Biophysics, Russian Academy of Sciences, Pushchino, Moscow Region 142290, Russian Federation

[1]To whom correspondenceshould be addressed at Medical University of South Carolina, DD504 Drug Discovery Building, 70 President Street, MSC 140, Charleston, SC 29425. Fax: 843-876-2353. E-mail: jjlemasters@musc.edu

ABSTRACT

Acetaminophen (APAP) overdose causes hepatotoxicity involving mitochondrial dysfunction and c-jun N-terminal kinase (JNK) activation. Because the safe limit of APAP dosing is controversial, our aim was to evaluate the role of the mitochondrial permeability transition (MPT) and JNK in mitochondrial dysfunction after APAP dosing considered nontoxic by criteria of serum alanine aminotransferase (ALT) release and histological necrosis *in vivo*. C57BL/6 mice were given APAP with and without the MPT inhibitor, N-methyl-4-isoleucine cyclosporin (NIM811), or the JNK inhibitor, SP600125. Fat droplet formation, cell viability, and mitochondrial function *in vivo* were monitored by intravital multiphoton microscopy. Serum ALT, liver histology, total JNK, and activated phospho(p)JNK were also assessed. High APAP (300 mg/kg) caused ALT release, necrosis, irreversible mitochondrial dysfunction, and hepatocellular death. By contrast, lower APAP (150 mg/kg) caused reversible mitochondrial dysfunction and fat droplet formation in hepatocytes without ALT release or necrosis. Mitochondrial protein *N*-acetyl-*p*-benzoquinone imine adducts correlated with early JNK activation, but irreversible mitochondrial depolarization and necrosis at high dose were associated with sustained JNK activation and translocation to mitochondria. NIM811 prevented cell death and/or mitochondrial depolarization after both high and low dose APAP. After low dose, SP600125 decreased mitochondrial depolarization. In conclusion, low dose APAP produces reversible MPT-dependent mitochondrial dysfunction and steatosis in hepatocytes without causing ALT release or necrosis, whereas high dose leads to irreversible mitochondrial dysfunction and cell death associated with sustained JNK activation. Thus, nontoxic APAP has the potential to cause transient mitochondrial dysfunction that may synergize with other stresses to promote liver damage and steatosis.

Key words: APAP; hepatocytes; mitochondria; multiphoton microscopy; nontoxic dose

Acetaminophen (APAP) overdose can cause severe liver injury, including serum alanine aminotransferase (ALT) elevation, hepatic necrosis, and acute liver failure (Larson, 2007). APAP toxicity shows a threshold dose-dependence such that therapeutic doses are generally considered nontoxic. The threshold dose causing liver damage varies between individuals. Infants and adults who are malnourished, alcohol-exposed or taking certain cytochrome P450 (CYP450)-inducing drugs may have increased sensitivity to APAP hepatotoxicity (Berling *et al.*, 2012; Riordan and Williams, 2002; Zimmerman and Maddrey, 1995). The safe

limit of APAP for therapeutic indications is still controversial (Goyal *et al.*, 2012; Schilling *et al.*, 2010; Watkins *et al.*, 2006).

Although extensively studied, mechanisms of APAP-induced liver injury remain incompletely understood. Although most of the drug is conjugated and excreted as glucuronide or sulfate conjugates, a small portion of APAP is metabolically activated by CYP450 enzymes to the toxic reactive metabolite, *N*-acetyl-*p*-benzoquinone imine (NAPQI) (6). NAPQI can be detoxified by GSH but after an overdose excess NAPQI binds to cellular proteins and initiates toxicity (6).

APAP-induced liver cell damage *in vitro* and *in vivo* is predominantly oncotic necrosis rather than apoptosis (Gujral *et al.*, 2002). Mitochondria are a primary target of NAPQI (Tirmenstein and Nelson, 1989). Previous studies show that APAP overdose causes mitochondrial dysfunction, including respiratory inhibition, mitochondrial oxidant stress, and onset of the mitochondrial permeability transition (MPT), leading to loss of the mitochondrial membrane potential and decreased hepatic ATP levels (Hanawa *et al.*, 2008; Kon *et al.*, 2004). The MPT is an abrupt increase in the permeability of the mitochondrial inner membrane to molecules of less than about 1500 Daltons in molecular weight (Zoratti and Szabo, 1995). The MPT plays an important role in development of both necrotic and apoptotic cell death (Kim *et al.*, 2003). c-Jun N-terminal protein kinase (JNK), a mitogen-activated protein kinase (MAPK), undergoes sustained activation and translocation to mitochondria in mouse hepatocytes both *in vitro* and *in vivo* after APAP exposure (Gunawan *et al.*, 2006), and JNK activation is reported to mediate the APAP-induced MPT (Hanawa *et al.*, 2008).

Previous studies indicate that cyclosporin A (CsA) inhibits the MPT and attenuates APAP hepatotoxicity both *in vivo* and *in vitro* (Kon *et al.*, 2004; Masubuchi *et al.*, 2005; Reid *et al.*, 2005). NIM811 is a nonimmunosuppressive derivative of CsA that inhibits the MPT equivalently to CsA in isolated mitochondria, cultured hepatocytes, and liver grafts after transplantation (Theruvath *et al.*, 2008; Waldmeier *et al.*, 2002). Because of controversies regarding the safe upper limit for APAP dosing, we investigated the possibility that APAP might cause MPT-dependent, NIM811-sensitive mitochondrial dysfunction at doses of APAP not causing overt hepatic damage. Using an *in vivo* mouse model of APAP hepatotoxicity and multiphoton microscopy, we show that APAP can cause reversible mitochondrial depolarization that is blocked by NIM811 at doses below the threshold causing hepatocellular death, hepatic necrosis, and transaminase release. This reversible mitochondrial depolarization is associated with transient JNK activation and translocation to mitochondria.

MATERIALS AND METHODS

Animals. Male C57BL/6 mice (8–9 weeks) were purchased from Jackson Laboratories (Bar Harbor, Maine). Mice were fasted overnight and then treated with vehicle (warm saline) or APAP (75–300 mg/kg, i.p.). NIM811 (Novartis, Basel, Switzerland; 10 mg/kg) or its vehicle (8% Cremophor EL [Sigma-Aldrich, St. Louis, Missouri], 8% ethanol in distilled water) was gavaged 1 h before APAP. In some experiments, the JNK inhibitor SP600125 (10 mg/kg, Sigma-Aldrich) or its vehicle (8.3% DMSO in normal saline) was injected (i.p.) 2 h after APAP. Animal protocols were approved by the Institutional Animal Care and Use Committee.

Alanine aminotransferase. At 6 and 24 h after vehicle or APAP injection, mice were anesthetized with ketamine/xylazine (100 mg/kg/, xylazine, i.p.), and blood was collected from the inferior vena cava. Serum ALT was measured using a commercial kit (Pointe Scientific, Canton, Michigan).

Histology. Livers were fixed by immersion in 4% buffered paraformaldehyde. Area percent of necrosis was quantified in hematoxylin and eosin (H&E)-stained paraffin sections (IP Lab, BD Biosciences, Rockville, Maryland). To assess steatosis, livers were frozen, sectioned and stained with Oil-Red-O.

Isolation of subcellular fractions and Western blotting. Mouse liver mitochondria and cytosolic fractions were isolated by differential centrifugation, as described (Bajt *et al.*, 2011). Western blotting was performed using rabbit anti-JNK and anti-phospho-JNK antibodies (Cell Signaling Technology, Danvers, Massachusetts) (Bajt *et al.*, 2011). Mitochondrial protein adducts were measured using HPLC with electrochemical detection, as described (McGill *et al.*, 2012b).

Loading of fluorescent probes. At 6 and 24 h after vehicle or APAP injection, mice were anesthetized with ketamine/xylazine and connected to a small animal ventilator via a respiratory tube (20-gauge catheter) inserted into the trachea. Green-fluorescing rhodamine 123 (Rh123, 2 μmol/mouse, mitochondrial ΔΨ indicator) (Lemasters and Ramshesh, 2007; Theruvath *et al.*, 2008) plus red-fluorescing propidium iodide (PI; 0.4 μmol/mouse, cell death indicator) (Shi *et al.*, 2012) or green-fluorescing 4,4-difluoro-1,3,5,7,8-pentamethyl-4-bora-3a,4a-diaza-s-indacene (BODIPY493/503, 0.4 μmol/mouse, lipid labeling agent) (Zhong *et al.*, 2014) plus red-fluorescing tetramethylrhodamine methylester (TMRM, 2 μmol/mouse, ΔΨ indicator) (Lemasters and Ramshesh, 2007) were infused via polyethylene-10 tubing inserted into the femoral vein over 10 min.

Intravital multiphoton microscopy. After infusion of fluorescent probes, individual mice were laparotomized and placed in a prone position. The liver was gently withdrawn from the abdominal cavity and placed over a No. 1.5 glass coverslip mounted on the stage of an inverted Olympus Fluoview 1000 or 1200 MPE multiphoton microscope (Olympus, Center Valley, Pennsylvania) equipped with a 25 × 1.05 NA water immersion or 30 × 1.05 N.A. silicone oil objective lens and a Spectra Physics Mai Tai Deep Sea tunable multiphoton laser (Newport, Irvine, California). Rh123 and PI fluorescence was imaged simultaneously using 820-nm multiphoton excitation. In other experiments, BODIPY and TMRM fluorescence was imaged using 920-nm multiphoton excitation. During image acquisition, the respirator was turned off 5–10 s to eliminate breathing movement artifacts. In some experiments, *z*-stacks of green and red fluorescence images were collected from planes 5.0 μm apart. Unless otherwise stated, images were collected 25 μm from the liver surface. Pericentral areas were identified by the sinusoidal configuration. Images in 10 random fields were analyzed using IP Lab. Nonviable PI-positive cells were also counted in 10 random fields per liver.

Statistical analysis. Data are presented as means ± standard error. Differences between groups were analyzed by ANOVA followed by Tukey's multiple comparison procedure using $P < .05$ as the criterion of significance.

RESULTS

High but Not Low APAP Causes Macroscopic Liver Injury and ALT Release That Is Inhibited by NIM811

After vehicle treatment at 6 and 24 h, gross liver appearance was normal and indistinguishable from untreated mice. After

300 mg/kg APAP, livers became pale and mottled at 6 h with frank hemorrhage at 24 h. However, after 150 mg/kg APAP with and without NIM811 pretreatment, gross liver appearance was not different from vehicle at both 6 and 24 h. NIM811 pretreatment decreased gross liver injury after 300 mg/kg APAP at both 6 and 24 h. However, some increased pallor remained, especially at 24 h (Figure 1A and not shown).

Serum ALT, an indicator of liver injury, was 30–35 U/l after vehicle treatment at 6 and 24 h, which was indistinguishable from untreated mice (Figs. 1B and C). After 75 and 150 mg/kg APAP with and without NIM811 treatment, ALT remained unchanged. After 300 mg/kg APAP, ALT increased markedly to 5104 and 10 526 U/l at 6 and 24 h, respectively. When mice were pretreated with NIM811, ALT after 300 mg/kg APAP decreased to 1350 and 2947 U/l at 6 and 24 h, representing protection by more than 70% (Figs. 1B and C).

High Dose but Not Low Dose APAP Causes Hepatic Necrosis That Is Partially Blocked by NIM811

After vehicle, liver histology after 6 and 24 h was normal and indistinguishable from untreated mice (Figure 2 and not shown). After 300 mg/kg APAP, areas of pericentral necrosis developed at both 6 and 24 h (Figure 2, arrows). Hemorrhagic areas became prominent after 24 h (Figure 2, asterisks). NIM811 pretreatment decreased hepatic necrosis after 300 mg/kg APAP from 23.3% to 2.1% at 6 h and from 50.9% to 4.5% at 24 h

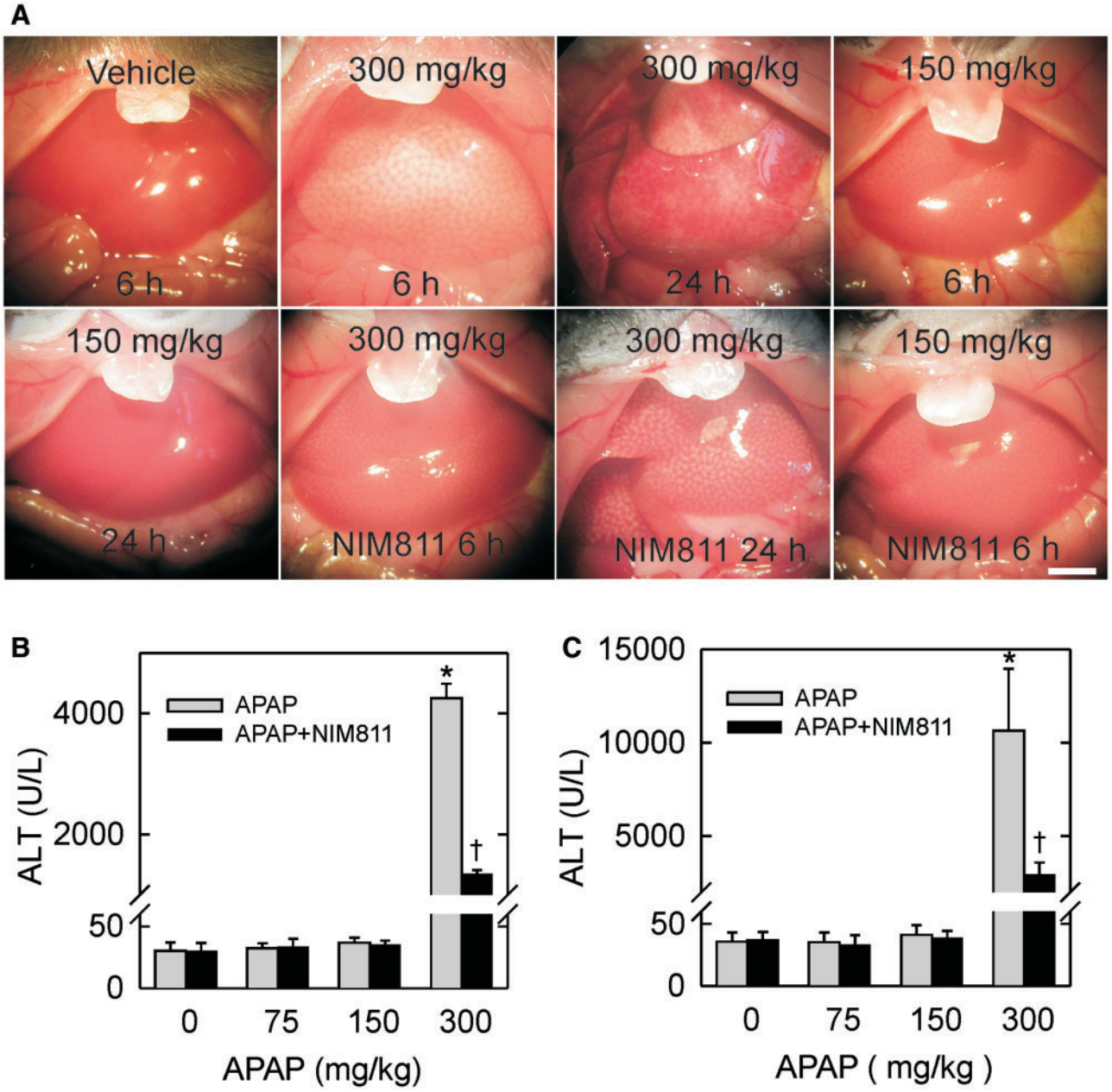

FIG. 1. Low dose acetaminophen (APAP) does not cause gross liver changes and aminotransferase (ALT) release. Mice were administered vehicle or APAP at low (75, 150 mg/kg) and high (300 mg/kg) doses. NIM811 (10 mg/kg) or vehicle was gavaged 1 h before APAP. In (A), photographs of livers were taken before tissue harvest at 6 and 24 h after vehicle or APAP injection. Bar is 3 mm. In (B) and (C), serum ALT was measured at 6 and 24 h, separately. *$P < .05$ versus vehicle; †$P < .05$ versus 300 mg/kg APAP.

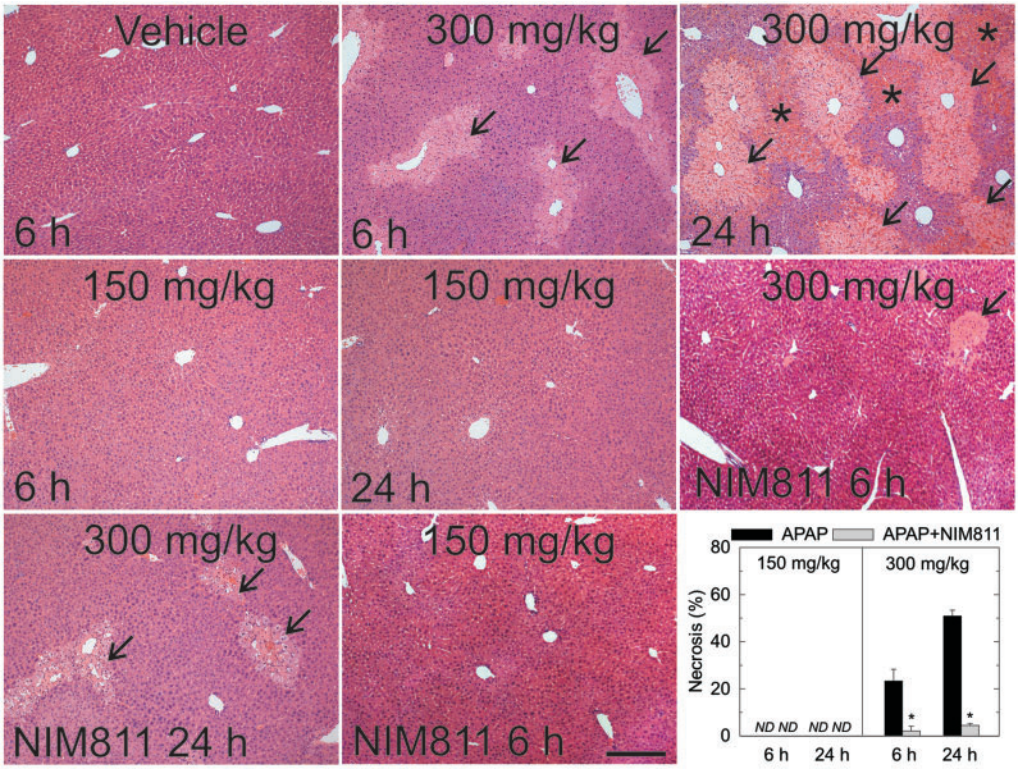

FIG. 2. High dose but not low dose acetaminophen (APAP) causes liver necrosis. Mice were treated with vehicle, NIM811 and/or APAP, as described in Figure 1, and necrosis was assessed by H&E histology. Black arrows identify necrotic areas. Asterisks (*) identify hemorrhage. Bar is 250 μm. Area percent of necrosis was quantified in liver sections by image analysis of 10 random fields per liver (lower right panel). Necrosis in vehicle and 75 mg/kg APAP groups was absent and not plotted. ND, not detectable; *$P < .05$.

(Figure 2, lower right panel). By contrast after 75 and 150 mg/kg APAP with and without NIM811 pretreatment, liver architecture remained completely normal.

High Dose APAP Causes Mitochondrial Depolarization and Cell Death In Vivo at 6 h

At 6 h after vehicle, intravital multiphoton microscopy revealed punctate green Rh123 fluorescence in virtually all hepatocytes, indicating polarization of mitochondria (Figure 3A, far left). Cytosolic and nuclear areas had little green fluorescence. Red PI labeling of nuclei signifying cell death was absent. By contrast at 6 h after 300 mg/kg APAP, Rh123 fluorescence became diffuse and dim in pericentral hepatocytes (Figure 3A far right, dashed line), indicating release of mitochondrial Rh123 due to depolarization of mitochondria. Additionally within areas with depolarized mitochondria, many nuclei became labeled with red-fluorescing PI, which identified nonviable hepatocytes (Figure 3A far right, arrows). Overlays of green and red images showed that in every instance PI-labeled hepatocytes contained depolarized mitochondria, as evidenced by dim, diffuse green Rh123 fluorescence. However, many other hepatocytes with dim, diffuse Rh123 fluorescence had not yet labeled with PI. These results showed that at 6 h after high dose (300 mg/kg) APAP, mitochondrial depolarization occurred in pericentral hepatocytes and that this depolarization preceded onset of cell death.

Low Dose APAP Causes Hepatocellular Mitochondrial Dysfunction In Vivo at 6 h

At 6 h after 150 mg/kg APAP, many pericentral hepatocytes showed dim, diffuse Rh123 fluorescence, indicating mitochondrial depolarization (Figure 3A middle right, dashed line). Other hepatocytes had diffuse but relatively bright green Rh123 fluorescence, most likely indicating recent depolarization of mitochondria, because Rh123 fluorescence after release from mitochondria initially increases due to unquenching prior to eventual diffusion of Rh123 outside the cells (Nieminen *et al.*, 1990). Despite consistent pericentral mitochondrial depolarization, PI labeling of nuclei was very rare, indicating the absence of cell death. These results show that at 6 h after 150 mg/kg APAP, mitochondrial depolarization occurred in pericentral areas without cell death. After 75 mg/kg APAP, by contrast, mitochondria in virtually all hepatocytes remained polarized and were indistinguishable from the vehicle-treated group (Figure 3A middle left).

Progression of Mitochondrial Depolarization and Cell Death at 24 h After High Dose APAP and Recovery of Mitochondrial Dysfunction after Low Dose

Livers were also imaged by intravital multiphoton microscopy at 24 h after treatment with 75–300 mg/kg APAP. After high dose (300 mg/kg) APAP, loss of Rh123 fluorescence indicating mitochondrial depolarization became more widespread than after 6 h and remained confined to pericentral regions (Figure 3B far right, dashed line). PI-labeled nuclei also increased and were again confined within regions of mitochondrial depolarization (Figure 3B far right, arrows).

At 24 h after lower dose (150 mg/kg) APAP, Rh123 fluorescence was bright and punctate throughout the liver lobule, indicating that mitochondria of pericentral hepatocytes that were depolarized at 6 h had now repolarized at 24 h (Figure 3B middle right). Additionally, PI labeling of nuclei was very rare. Overall, intravital images at 24 h after 150 mg/kg APAP were

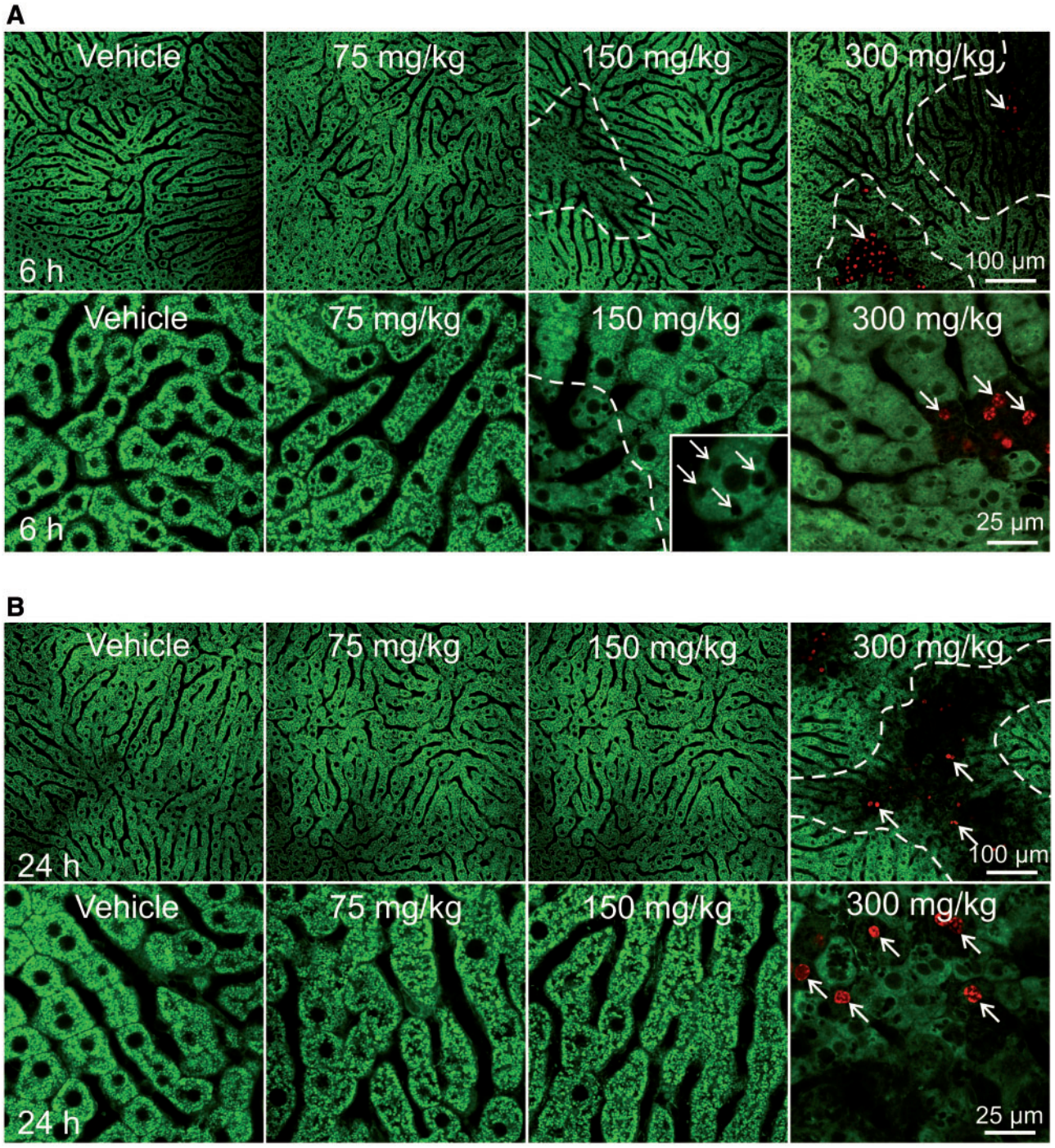

FIG. 3. Low dose APAP causes reversible mitochondrial depolarization without cell death, whereas high dose APAP causes sustained mitochondrial dysfunction accompanied by cell death. Mice were treated with vehicle or APAP, as described in Figure 1. Intravital multiphoton microscopy was performed after infusion of Rh123 and PI. Shown are representative overlay images of green Rh123 and red PI fluorescence collected from livers at 6 h (A) and 24 h (B) after vehicle or APAP treatment. Top and bottom rows show low and high power images, respectively. Punctate labeling with Rh123 signifies mitochondrial polarization, whereas dim diffuse Rh123 staining denotes mitochondrial depolarization (dashed line). Nuclear PI labeling signifies cell death (arrows). The higher magnification inset in (A, bottom middle right) illustrates dark voids (arrows) in the diffuse Rh123 fluorescence.

indistinguishable from vehicle treatment (Figure 3B middle right). Moreover, depolarization without PI labeling after 6 h but not after 24 h did not change as images were collected at different depths into the tissue (Supplementary Fig. 1). Similarly, intravital multiphoton images of livers at 24 h after 75 mg/kg APAP were indistinguishable from vehicle treatment (Figure 3B middle left).

Mitochondrial Protein Adducts and Activation and Mitochondrial Translocation of JNK After APAP

Formation of mitochondrial protein adducts is an important initiating event for mitochondrial dysfunction (Jaeschke *et al.*, 2012). To assess if mitochondrial protein adducts correlated with cell necrosis, adducts were measured after treatment with various doses of APAP at 1 h, a time corresponding to the peak

of adduct formation (McGill *et al.*, 2012b). Mitochondrial APAP protein adducts were clearly detectable after the 150 and 300 mg/kg dose but not after 75 mg/kg (Figure 4A). Mitochondrial dysfunction and oxidant stress induce JNK activation (Hanawa *et al.*, 2008). To assess if mitochondrial protein adduct formation correlates with JNK activation, total JNK, and phosphorylated JNK (pJNK) levels were measured in cytosolic and mitochondrial fractions (Figure 4B). After the high dose (300 mg/kg) of APAP, pJNK levels increased in hepatic cytosol and mitochondria after both 2 and 6 h (Figure 4B). By contrast, after 150 mg/kg APAP, pJNK increased in the cytosol and to a small extent in mitochondria only after 2 h. After 6 h, total JNK was unchanged in the cytosol, but pJNK had disappeared in both fractions (Figure 4A). No JNK activation or mitochondrial translocation was observed after 75 mg/kg APAP (data not shown). Thus, mitochondrial protein adduct formation correlated with the transient early JNK activation and pJNK translocation to the mitochondria and with the transient mitochondrial depolarization at 6 h. However, sustained JNK activation and mitochondrial translocation, as observed after the 300 mg/kg dose, was necessary to induce persistent mitochondrial depolarization and cell necrosis.

Protection Against Mitochondrial Depolarization by NIM811

Because of previous reports that APAP induces the MPT, which in turn causes mitochondrial depolarization, we investigated whether the MPT inhibitor NIM811 would decrease hepatic mitochondrial depolarization *in vivo* after APAP treatment. After high dose (300 mg/kg) APAP with NIM811 pretreatment, substantially fewer pericentral hepatocytes displayed dim, diffuse Rh123 fluorescence at both 6 and 24 h (Figure 5 middle and far right, dashed line). PI labeling of nuclei also decreased (Figure 5 far right, arrows). After low dose (150 mg/kg) APAP, NIM811 prevented mitochondrial depolarization virtually completely at 6 h,

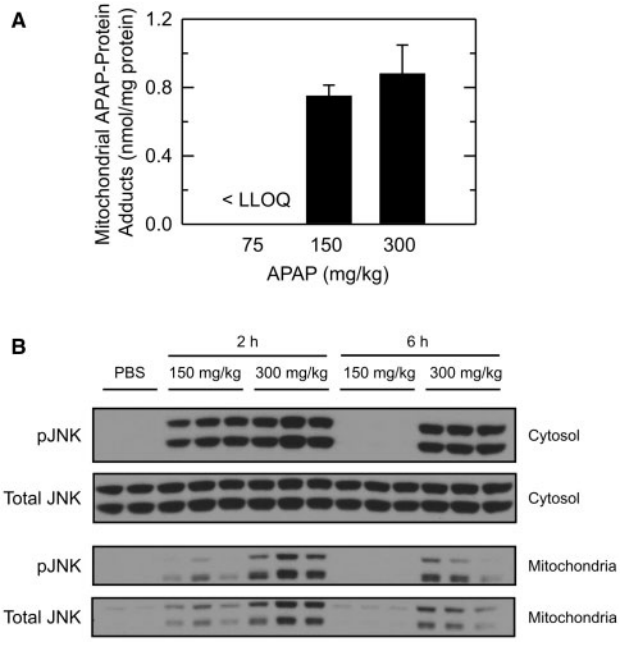

FIG. 4. APAP-induced mitochondrial protein adducts and JNK activation. Mice were treated with APAP, as described in Figure 1. In (A), mitochondrial protein adducts were measured by HPLC after 1 h. In (B), pJNK and total JNK in hepatic cytosolic and mitochondrial fractions were determined by Western analysis after 2 and 6 h. LLOQ, lower limit of quantification; PBS, saline.

and all hepatocytes displayed bright punctate Rh123 fluorescence, which was indistinguishable from NIM811 alone and vehicle alone (Figure 5 middle and far left, compare to Figure 3).

Protection Against Mitochondrial Depolarization by JNK Inhibition

We then assessed the effect of JNK inhibition with SP600125 on early mitochondrial depolarization after low dose APAP. Since the vehicle for SP600125 contained DMSO and DMSO can alter the metabolism and hence toxicity of APAP (Park *et al.*, 1988; Yoon *et al.*, 2006), we administered SP600125 2 h after APAP to avoid vehicle issues. With vehicle treatment, 150 mg/kg APAP still induced dim and diffuse of Rh123 fluorescence in pericentral area at 6 h, indicating mitochondrial depolarization (Fig. 6 left, dashed line). However, SP600125 substantially decreased mitochondrial depolarization at 6 h (Figure. 6 left, dashed line, compared with right). In some instances, pericentral mitochondrial depolarization was prevented completely by SP600125 (Figure 6, lower right).

Quantitation of Mitochondrial Depolarization and Cell Death

Rh123 fluorescence and PI labeling were quantified for the various treatment groups. After vehicle, no depolarization of mitochondria occurred, as indicated by the absence of diffuse Rh123 fluorescence, and no cells were nonviable by nuclear PI labeling (Figure 7). After 300 mg/kg APAP (high dose), 58.3% of hepatocytes (area percent) displayed mitochondrial depolarization at 6 h, which increased to 83.9% at 24 h. NIM811 pretreatment decreased depolarization to 16.4% and 27.3% at 6 and 24 h, respectively (Fig. 7A). After 300 mg/kg APAP, nuclear PI labeling increased from 0/high power field (HPF) after vehicle to 6.5/HPF at 6 h. Cell killing increased further to 8.8/HPF at 24 h. NIM811 pretreatment before 300 mg/kg APAP decreased nuclear PI labeling to 0.07 and 0.5/HPF at 6 and 24 h (Figure 7B). After low dose (150 mg/kg) APAP, NIM811 decreased depolarization areas from 15.7% to 0.4% at 6 h ($P < .05$). JNK inhibition with SP600125 also decreased depolarization areas at 6 h but to a lesser extent from 14.3% to 5% ($P < .05$) (Figure 7C). Depolarization was absent at 24 h after low dose APAP administration with and without NIM811 pretreatment. Cell killing (PI labeling) was absent at both 6 and 24 h after low dose APAP administration with and without NIM811 pretreatment.

Low Dose APAP Causes Reversible Hepatic Steatosis

After mitochondrial depolarization from APAP, round dark voids frequently developed within the diffuse cytoplasmic fluorescence of Rh123 (Figure 3A, bottom middle right inset, arrows). To determine whether these dark voids represented fat droplets, we stained frozen sections with Oil-Red-O. After vehicle treatment, Oil-Red-O-stained fat droplets were small and sparse (Figure 8A left). At 6 h after lower dose (150 mg/kg) APAP, numerous Oil-Red-O-stained fat droplets became evident in pericentral hepatocytes (Figure 8A middle), but by 24 h the livers had recovered from this steatosis, and fat droplets were again small and sparse (Figure 8A right). Thus, lower dose (150 mg/kg) APAP caused both pericentral mitochondrial depolarization and steatosis, which was transient and not accompanied by cell death, necrosis, or ALT release.

Hepatic Steatosis Caused by Low Dose APAP Is Associated with Mitochondrial Depolarization

To assess the relationship of steatosis with mitochondrial depolarization after low dose (150 mg/kg) APAP, mice were infused simultaneously with $\Delta\Psi$-indicating TMRM and lipid droplet-indicating BODIPY. After vehicle, virtually all hepatocytes

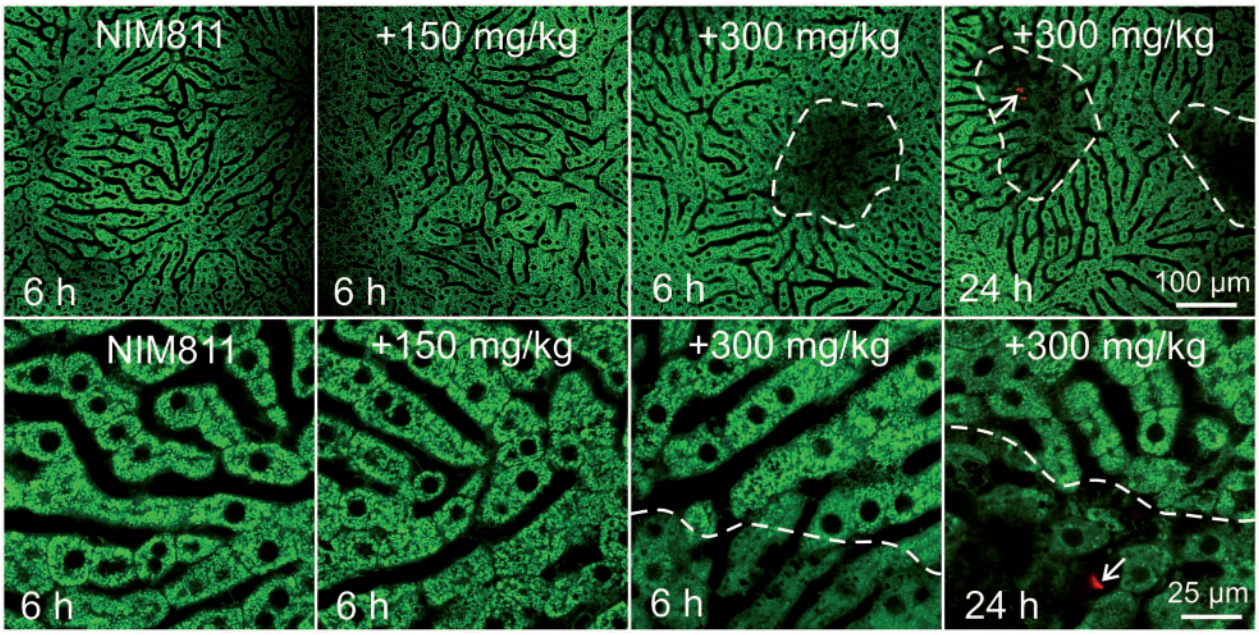

FIG. 5. NIM811 decreases hepatocellular cell death and/or mitochondrial depolarization after both low and high dose APAP. Mice were treated with vehicle, NIM811 and APAP, as described in Figure 1, and multiphoton microscopy was performed. As indicated, shown are representative overlay images of green Rh123 and red PI fluorescence collected from NIM811-pretreated livers at 6 and 24 h after vehicle and different doses of APAP. Punctate labeling of Rh123 signifies mitochondrial polarization, whereas diffuse cellular staining denotes mitochondrial depolarization (dashed line). Nuclear PI labeling signifies cell death (arrows).

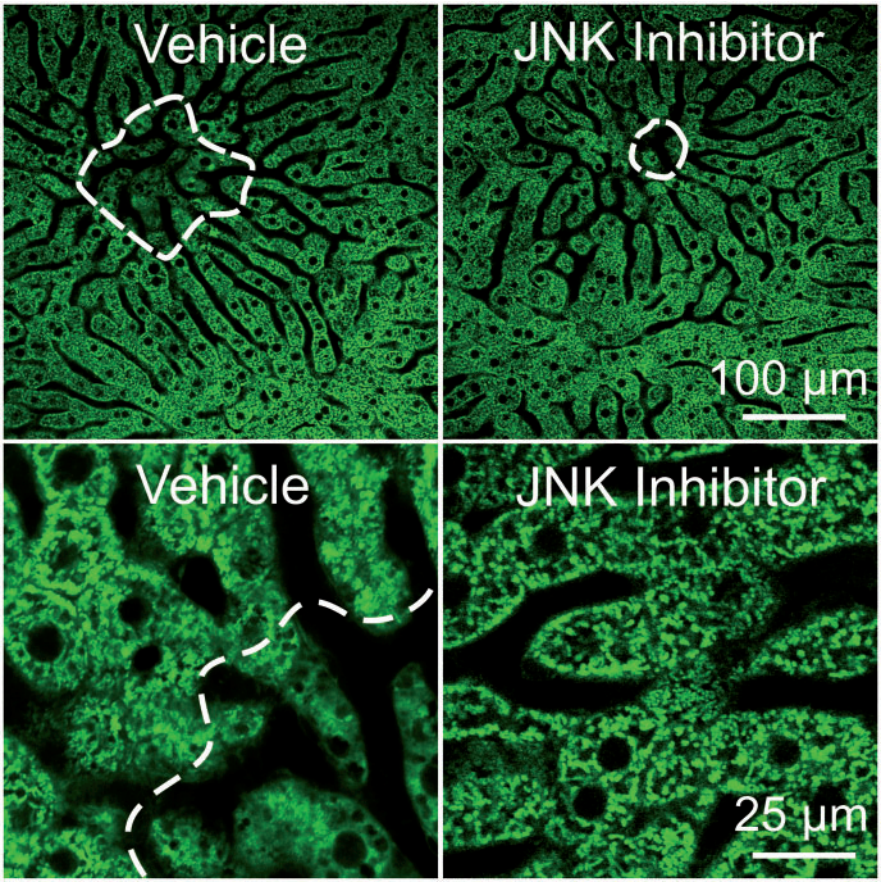

FIG. 6. The JNK inhibitor SP600125 decreases hepatocellular mitochondrial depolarization after low dose APAP. Mice were administered vehicle or 150 mg/kg APAP. JNK inhibitor (SP600125, 10 mg/kg) or vehicle was injected 2 h after APAP. Multiphoton microscopy was performed at 6 h after APAP. As indicated, shown are representative overlay images of green Rh123 and red PI fluorescence collected from livers at 6 h after low dose APAP. Punctate labeling of Rh123 signifies mitochondrial polarization, whereas diffuse cellular staining denotes mitochondrial depolarization (dashed line).

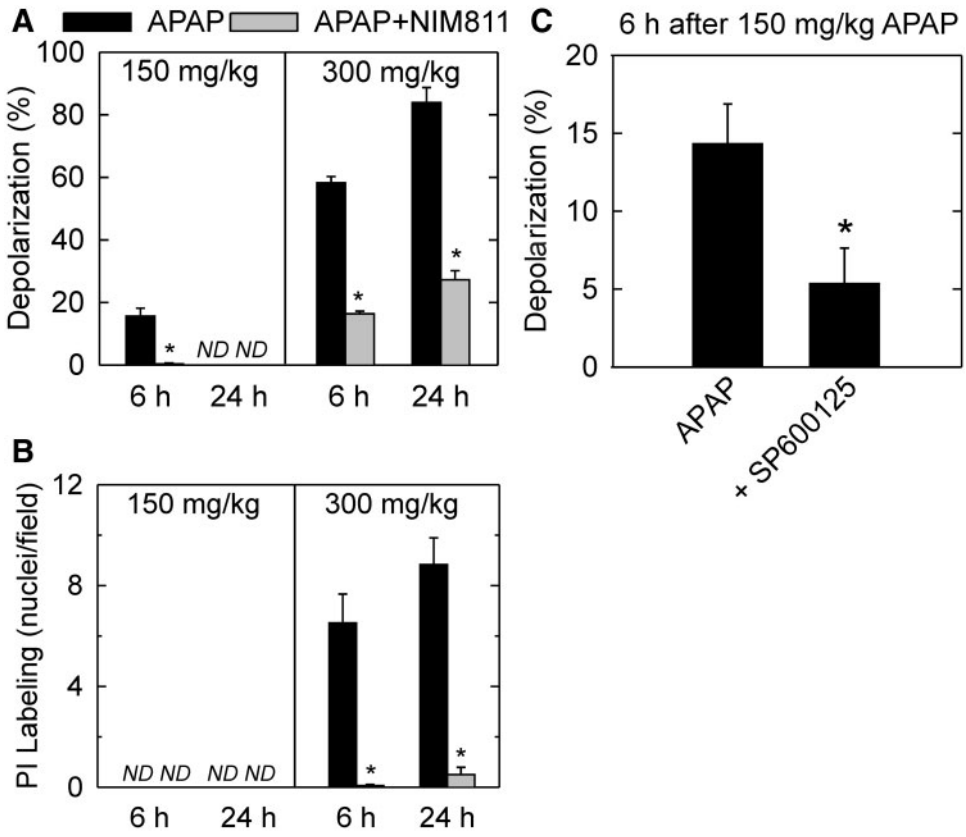

FIG. 7. Protection by NIM811 and SP600125 against depolarization and cell death induced by APAP. Mice were treated with vehicle, NIM811, SP600125 and/or APAP, as described in Figures 5 and 6. Percent area of mitochondrial depolarization is plotted for various treatment groups for 3–4 livers per group (A and C). PI-labeled nuclei were also counted (B). N.D., not detectable; *$P < .05$

displayed punctate, red fluorescence of TMRM, indicating mitochondrial polarization (Figure 8B top left). Fat droplets labeled by green-fluorescing BODIPY were small and relatively sparse. At 6 h after low dose (150 mg/kg) APAP, TMRM fluorescence in pericentral hepatocytes became diffuse with development of round dark voids, as observed with Rh123 labeling (Figure 8B bottom right, compare with Figure 3). BODIPY revealed that these dark voids coincided with fat droplets inside hepatocytes with depolarized mitochondria (Figure 8B top and bottom middle). NIM811 decreased both mitochondrial depolarization and steatosis at 6 h (Figure 8B top right). At 24 h after 150 mg/kg APAP, mitochondria repolarized (as observed with Rh123), and the number of BODIPY stained green fat droplets decreased (Figure 8B bottom right). The percent of BODIPY stained area was quantified after various treatments. After vehicle, 2.1% of area was labeled with BODIPY, which increased to 6.4% at 6 h after 150 mg/kg APAP and then decreased to 1.7% at 24 h. NIM811 pretreatment decreased steatosis area to 3.0% at 6 h (Fig. 8C).

DISCUSSION

In vivo in mice, hepatic APAP-protein adduct formation peaks at 0.5–1 h after APAP treatment (23) followed some hours later by mitochondrial dysfunction and cell death. Liver damage assessed by ALT release begins at about 3 h after APAP and increases progressively to peak after 12–24 h (Bajt *et al.*, 2008). If APAP toxicity is not fatal, ALT typically returns to normal within 4 days (Bhushan *et al.*, 2014). Our data confirm this time-dependent hepatotoxicity. After 300 mg/kg APAP, ALT increased, and macroscopic changes of liver appearance (mottling, pallor) and outright necrosis developed at 6 h, which became more severe by 24 h (Figs. 1 and 2). By contrast, 75 and 150 mg/kg APAP did not induce macroscopic liver changes, increase ALT or cause pericentral necrosis in agreement with previous reports (Heinloth *et al.*, 2004). Thus, 75 and 150 mg/kg doses of APAP were not toxic by conventional indices of hepatic injury damage, whereas 300 mg/kg dose was unequivocally hepatotoxic.

Previous studies in cultured mouse hepatocytes show that toxic doses of APAP induce mitochondrial depolarization and inner membrane permeabilization (Kon *et al.*, 2004, 2010; Reid *et al.* 2005). To visualize changes of hepatic mitochondrial function *in vivo* after APAP, we used intravital multiphoton microscopy. Our studies revealed that mitochondrial depolarization and cell death developed in pericentral hepatocytes within 6 h after 300 mg/kg APAP and became more severe after 24 h (Figs. 3 and 6), indicating that this toxic dose of APAP caused sustained and irreversible mitochondrial dysfunction *in vivo*. Unexpectedly, mitochondrial depolarization in pericentral hepatocytes also occurred in mice at 6 h after treatment with 150 mg/kg, which was a "nontoxic" dose of APAP not causing necrosis or enzyme release. Despite this mitochondrial depolarization, nuclear PI labeling after 150 mg/kg APAP was not observed at any time point examined. Indeed, mitochondrial depolarization observed after 6 h spontaneously reversed after 24 h (Figs. 3 and 6). Mitochondrial images at different distances from the liver surface confirmed these findings (Supplementary Fig. 1). Thus, 150 mg/kg APAP caused transient mitochondrial dysfunction that reversed spontaneously and did not induce cell death.

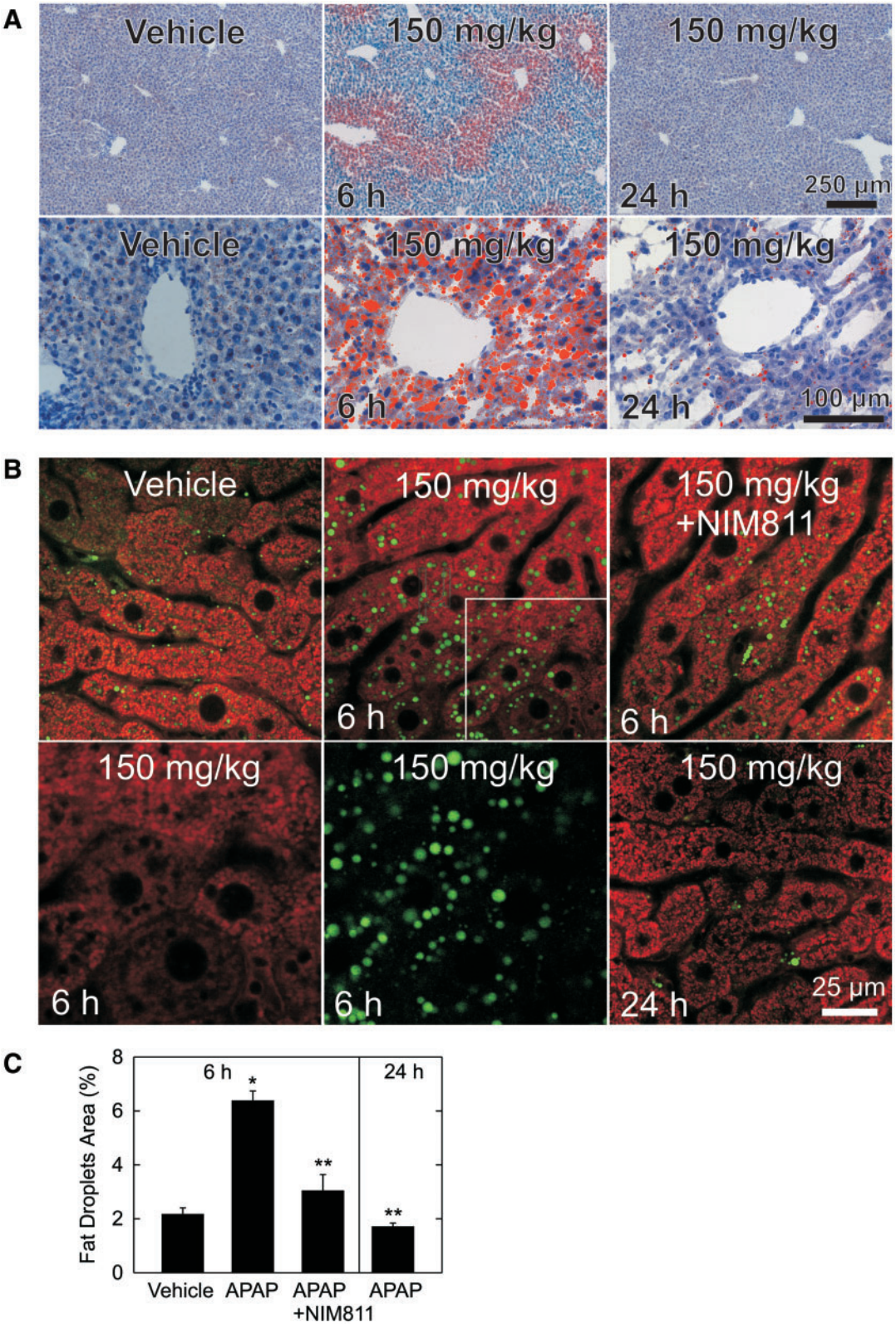

FIG. 8. Low dose APAP induces transient hepatic steatosis. A, Mice were administered vehicle or 150 mg/kg APAP. Steatosis was assessed by oil red O staining after vehicle and at 6 and 24 h after APAP. Top and bottom rows are low and high power images, respectively. B, Mice were treated with vehicle, NIM811 and APAP, as described in Figure 1. TMRM and BODIPY were infused, and intravital multiphoton microscopy was performed. Shown are representative images of green BODIPY and red TMRM fluorescence collected from livers after vehicle, 6 h after APAP, 6 h after APAP plus NIM811, and 24 h after APAP. Bottom left and middle are the separate red and green channels of the area shown by the inset in the top middle. Note that green BODIPY labeling of fat droplets coincided with round dark cytoplasmic voids in the TMRM fluorescence. In (C), area percent of BODIPY staining was quantified. *$P < .05$ versus vehicle; **$P < .05$ versus 6 h after 150 mg/kg APAP.

Mitochondrial APAP protein adduct formation is thought to trigger an initial oxidant stress, which can induce JNK activation (Saito *et al.*, 2010a). Activated pJNK translocates to mitochondria during APAP hepatotoxicity, an event that appears to enhance ROS generation and precipitate the MPT and cell death (Hanawa *et al.*, 2008; Saito *et al.*, 2010a). Our data confirmed that early JNK activation and mitochondrial pJNK translocation occurred at 2 h only after a dose of APAP that triggered relevant mitochondrial protein adduct formation. Early JNK activation at 2 h correlated with mitochondrial depolarization at 6 h after these doses. At the lower nontoxic APAP dose, JNK activation, mitochondrial pJNK translocation, and mitochondrial depolarization were transient, reversible events. Consistent with previous *in vitro* studies (Kon *et al.*, 2004, 2010), pilot studies failed to show any mitochondrial depolarization after 2 h (data not shown), indicating that JNK activation and mitochondrial translocation at 2 h occurred prior to mitochondrial depolarization at 6 h. Nonetheless, transient JNK activation after the lower nontoxic APAP dose contributed to transient mitochondrial depolarization, since JNK inhibition with SP600125 decreased this depolarization by almost two-thirds (Figs. 6 and 7). Sustained JNK activation and sustained presence of pJNK in the mitochondria appears to be necessary for permanent mitochondrial depolarization and development of cell necrosis. This is consistent with the hypothesis that prolonged JNK activation is needed to amplify the mitochondrial oxidant stress that triggers the MPT and causes cell necrosis (Hanawa *et al.*, 2008; Saito *et al.*, 2010a). The main difference between the nontoxic 150 mg/kg dose and the toxic 300 mg/kg dose is not the initial depletion of hepatic GSH but the recovery of these GSH levels, which is substantially accelerated after the lower dose (23). A faster recovery of hepatic GSH during the most critical phase of mitochondrial oxidant stress and peroxynitrite formation was shown to protect dramatically against APAP-induced cell death (Saito *et al.*, 2010 b). These findings stress the importance of prolonged JNK activation for permanent mitochondrial depolarization and emphasize possible therapeutic targets to block this process.

No mitochondrial depolarization was observed after administration of 75 mg/kg APAP (Figure 3), which might be considered the real maximal safe dose of APAP for mice. Nonetheless, GSH can become maximally depleted within 1 h leading to NAPQI protein adduct formation within 2 h even at APAP doses below those causing hepatic necrosis (Reid *et al.*, 2005). Thus after treatment with 75 mg/kg APAP, we cannot not exclude the possibility that mitochondrial dysfunction happened at an earlier time and had already recovered by 6 h when we first performed our intravital multiphoton experiments. A dose of 75 mg/kg corresponds approximately to the accepted 4 g daily limit for APAP use by humans, which supports current clinical recommendations (Schilling *et al.*, 2010). However, mice metabolize APAP more rapidly than humans (McGill *et al.*, 2012 a). Thus, doses in humans less than 4 g might still cause transient mitochondrial dysfunction that synergizes with other hepatocellular stresses to cause hepatic necrosis and enzyme release.

Previous studies implicate the MPT in the mechanism of APAP-induced hepatotoxicity (Kon *et al.*, 2004; Masubuchi *et al.*, 2005; Reid *et al.*, 2005). The MPT inhibitor CsA delays APAP-induced cell killing in cultured mouse hepatocytes and decreases hepatic injury in APAP-treated mice (Kon *et al.*, 2004, 2010; Masubuchi *et al.*, 2005). NIM811, a nonimmunosuppressive CsA analog, blocks the MPT similarly to CsA and protects *in vivo* in several experimental models of hepatic injury, including cold storage/reperfusion injury, small-for-size liver transplantation, CCl_4-induced liver fibrosis, hepatectomy, and cholestasis (Rehman *et al.*, 2008; Theruvath *et al.*, 2008; Zhong *et al.*, 2007, 2008). Here using intravital multiphoton microscopy, we showed that NIM811 substantially decreased mitochondrial depolarization and cell death at both 6 h and 24 h after treatment of mice with 300 mg/kg APAP (Figs. 5 and 6), results that confirm and extend the conclusion that the MPT is a principal mechanism contributing to APAP-induced liver injury. NIM811 also blocked transient mitochondrial depolarization at 6 h after 150 mg/kg APAP (Figs. 5 and 6). Thus, reversible mitochondrial injury after low dose APAP was still related to permeability transition (PT) pore activity. Similar reversible CsA-sensitive mitochondrial depolarization occurs in somatosensory cortex in an *in vivo* mouse stroke model (Liu and Murphy, 2009). Moreover in isolated mitochondria, PT pore opening is well established to be reversible (Crompton, 1999). Thus, reversible PT pore opening likely explains the transient nature of mitochondrial dysfunction after administration of an otherwise nontoxic dose of APAP.

PT pores have 2 open conductance modes–a Ca^{2+}-activated and CsA-sensitive regulated mode associated with early PT pore opening and an unregulated mode occurring later, which does not require Ca^{2+} and is not inhibited by CsA (He and Lemasters, 2002). In cultured mouse hepatocytes, CsA and NIM811 delayed but did not prevent APAP-induced mitochondrial depolarization, indicating APAP initially induces a regulated MPT that is later superseded by an unregulated MPT (Kon *et al.*, 2004). Here, we found that cytoprotection by NIM811 persisted after 24 h of APAP administration (Figure 5). This is consistent with previous *in vivo* data showing protection in cyclophilin D-deficient mice after a dose of 200 mg/kg APAP (Ramachandran *et al.*, 2011). However, this protective effect disappeared when a dose of 600 mg/kg APAP was used (LoGuidice and Boelsterli, 2011). Thus, both *in vitro* and *in vivo* the MPT can be regulated after a moderate stress but is unregulated after a more severe stress. Our results suggest that NIM811 might have clinical value to prevent and even treat APAP-induced mitochondrial dysfunction and hepatotoxicity under certain conditions.

At 6 h after a lower "nontoxic" dose of APAP, round dark voids appeared in the cytoplasm of hepatocytes with depolarized mitochondria. Intravital multiphoton imaging of BODIPY identified these voids as lipid droplets, which oil red O staining of frozen sections confirmed (Figure 8A). However, lipid droplets disappeared at 24 h when mitochondria repolarized (Figure 8B). These findings are in agreement with reports that APAP induces hepatic steatosis in some individuals (Ramachandran and Kakar, 2009). A proposed mechanism for this steatosis is inhibition by NAPQI and oxidative stress of fatty acid oxidation enzymes located in the mitochondria matrix (Chen *et al.*, 2009). Indeed, acute mitochondrial dysfunction for a variety of reasons is well established to cause hepatic steatosis (Lemasters, 2013; Pessayre *et al.*, 2012). Protection by NIM811 against steatosis implies that PT pore opening is the cause of mitochondrial dysfunction after APAP and the consequent steatotic transformation of hepatocytes (Fig. 8B).

Mitochondrial depolarization is a strong signal inducing mitochondrial autophagy, or mitophagy (Kim and Lemasters, 2011; Youle and Narendra, 2011). Thus, MPT-dependent mitochondrial depolarization may underlie increased mitophagy after APAP, as recently reported (Ni *et al.*, 2012). Similarly, reversible mitochondrial depolarization leading to steatosis occurs after acute ethanol treatment of mice, which may also stimulate enhanced hepatic mitophagy (Ding *et al.*, 2010; Zhong *et al.*, 2014). Thus, mitochondrial depolarization may be a common event leading both to steatosis and mitophagy. However, once

cells lose viability, hepatocytes release their fat droplets, such that steatosis is never present in necrotic regions of the liver.

Legitimate concerns remain regarding the safe upper dose limit for APAP, currently listed at 4 g/day (Goyal *et al.*, 2012; Schilling *et al.*, 2010; Watkins *et al.*, 2006). Our data in mice showed that 150 mg/kg APAP did not induce ALT release, liver necrosis or macroscopic liver changes (Fig. 1 and 2). By these conventional criteria of hepatotoxicity in both mice and man, 150 mg/kg would be considered a safe dose. Nonetheless, we show that this dose causes transient mitochondrial depolarization, JNK activation, and steatosis (Figs. 3, 4, 7, and 8), which are adverse biological effects that might synergize with other hepatic stresses to produce more overt toxicity. The implication of our work to human hepatotoxicity is that the absence of transaminase release and hepatic necrosis does not necessarily rule out adverse liver effects at low APAP dosages. Thus, APAP in humans at less than 4 g may be safe for healthy people but still contribute to and possibly precipitate overt hepatotoxicity in patients with other hepatocellular stresses. For example in malnourished patients, transient mitochondrial dysfunction induced by low dose APAP may become magnified and lead to overt hepatic damage.

In conclusion, this study shows that even "nontoxic" doses of APAP that do not cause transaminase release and histological necrosis can nonetheless lead to transient hepatocellular mitochondrial dysfunction and steatosis. Unlike overdose-induced hepatotoxicity, the effects of subtoxic APAP are comparably mild and reversible and correlate with transient JNK activation and mitochondrial translocation. However in patients subjected to other stresses, APAP-induced transient mitochondrial dysfunction may lead to overt transaminase release and necrosis. Serial ingestion of APAP may compound this danger, because there may be inadequate time for hepatocytes to recover between dosings. Protection against mitochondrial dysfunction by the MPT inhibitor NIM811 implies that MPT onset plays an important role in mitochondrial dysfunction after both low and high dose APAP. These new findings suggest that even "nontoxic" doses of APAP can nonetheless trigger a transient stress on the mitochondria.

FUNDING

National Institutes of Health, (Grant / Award Number: "C06 RR015455," "DK037034," "DK073336," "DK102142", "P30 CA138313" and "5 P20 GM103542").

ACKNOWLEDGMENTS

This work was supported, in part, by Grants DK073336 and DK037034 to J.J.L. and Grant DK102142 to H.J. from the National Institutes of Health. Imaging facilities were supported, in part, by P30 CA138313 and 5 P20 GM103542 with animal facility support from Grant C06 RR015455.

SUPPLEMENTARY DATA

Supplementary data are available online at http://toxsci.oxfordjournals.org/.

REFERENCES

Bajt, M. L., Farhood, A., Lemasters, J. J., and Jaeschke, H. (2008). Mitochondrial bax translocation accelerates DNA fragmentation and cell necrosis in a murine model of acetaminophen hepatotoxicity. *J. Pharmacol. Exp. Ther.* **324**, 8–14.

Bajt, M. L., Ramachandran, A., Yan, H. M., Lebofsky, M., Farhood, A., Lemasters, J. J., and Jaeschke, H. (2011). Apoptosis-inducing factor modulates mitochondrial oxidant stress in acetaminophen hepatotoxicity. *Toxicol. Sci.* **122**, 598–605.

Berling, I., Anscombe, M., and Isbister, G. K. (2012). Intravenous paracetamol toxicity in a malnourished child. *Clin. Toxicol.* **50**, 74–76.

Bhushan, B., Walesky, C., Manley, M., Gallagher, T., Borude, P., Edwards, G., Monga, S. P., and Apte, U. (2014). Pro-regenerative signaling after acetaminophen-induced acute liver injury in mice identified using a novel incremental dose model. *Am. J. Pathol.* **184**, 3013–3025.

Chen, C., Krausz, K. W., Shah, Y. M., Idle, J. R., and Gonzalez, F. J. (2009). Serum metabolomics reveals irreversible inhibition of fatty acid beta-oxidation through the suppression of PPARalpha activation as a contributing mechanism of acetaminophen-induced hepatotoxicity. *Chem. Res. Toxicol.* **22**, 699–707.

Crompton, M. (1999). The mitochondrial permeability transition pore and its role in cell death. *Biochem. J.* **341(**Pt 2**)**, 233–249.

Ding, W. X., Li, M., Chen, X., Ni, H. M., Lin, C. W., Gao, W., Lu, B., Stolz, D. B., Clemens, D. L., and Yin, X. M. (2010). Autophagy reduces acute ethanol-induced hepatotoxicity and steatosis in mice. *Gastroenterology* **139**, 1740–1752.

Goyal, R. K., Rajan, S. S., Essien, E. J., and Sansgiry, S. S. (2012). Effectiveness of FDA's new over-the-counter acetaminophen warning label in improving consumer risk perception of liver damage. *J. Clin. Pharm. Ther.* **37**, 681–685.

Gujral, J. S., Knight, T. R., Farhood, A., Bajt, M. L., and Jaeschke, H. (2002). Mode of cell death after acetaminophen overdose in mice: apoptosis or oncotic necrosis? *Toxicol. Sci.* **67**, 322–328.

Gunawan, B. K., Liu, Z. X., Han, D., Hanawa, N., Gaarde, W. A., and Kaplowitz, N. (2006). c-Jun N-terminal kinase plays a major role in murine acetaminophen hepatotoxicity. *Gastroenterology* **131**, 165–178.

Hanawa, N., Shinohara, M., Saberi, B., Gaarde, W. A., Han, D., and Kaplowitz, N. (2008). Role of JNK translocation to mitochondria leading to inhibition of mitochondria bioenergetics in acetaminophen-induced liver injury. *J. Biol. Chem.* **283**, 13565–13577.

He, L., and Lemasters, J. J. (2002). Regulated and unregulated mitochondrial permeability transition pores: a new paradigm of pore structure and function? *FEBS Lett.* **512**, 1–7.

Heinloth, A. N., Irwin, R. D., Boorman, G. A., Nettesheim, P., Fannin, R. D., Sieber, S. O., Snell, M. L., Tucker, C. J., Li, L., Travlos, G. S., *et al.* (2004). Gene expression profiling of rat livers reveals indicators of potential adverse effects. *Toxicol. Sci.* **80**, 193–202.

Jaeschke, H., McGill, M. R., and Ramachandran, A. (2012). Oxidant stress, mitochondria, and cell death mechanisms in drug-induced liver injury: lessons learned from acetaminophen hepatotoxicity. *Drug Metab Rev.* **44**, 88–106.

Kim, I., and Lemasters, J. J. (2011). Mitophagy selectively degrades individual damaged mitochondria after photoirradiation. *Antioxid. Redox. Signal.* **14**, 1919–1928.

Kim, J. S., Qian, T., and Lemasters, J. J. (2003). Mitochondrial permeability transition in the switch from necrotic to apoptotic cell death in ischemic rat hepatocytes. *Gastroenterology* **124**, 494–503.

Kon, K., Kim, J. S., Jaeschke, H., and Lemasters, J. J. (2004). Mitochondrial permeability transition in acetaminophen-induced necrosis and apoptosis of cultured mouse hepatocytes. *Hepatology* **40**, 1170–1179.

Kon, K., Kim, J. S., Uchiyama, A., Jaeschke, H., and Lemasters, J. J. (2010). Lysosomal iron mobilization and induction of the mitochondrial permeability transition in acetaminophen-induced toxicity to mouse hepatocytes. *Toxicol. Sci.* **117**, 101–108.

Larson, A. M. (2007). Acetaminophen hepatotoxicity. *Clin. Liver Dis.* **11**, 525–548.

Lemasters, J. J. (2013). Hepatotoxicity due to mitochondrial injury. *In Drug-Induced Liver Disease*, 3rd ed. (N. Kaplowitz and L. Deleve, Eds.), pp. 85–100. Elsevier, Amsterdam.

Lemasters, J. J., and Ramshesh, V. K. (2007). Imaging of mitochondrial polarization and depolarization with cationic fluorophores. *Methods Cell Biol.* **80**, 283–295.

Liu, R. R., and Murphy, T. H. (2009). Reversible cyclosporin A-sensitive mitochondrial depolarization occurs within minutes of stroke onset in mouse somatosensory cortex in vivo: a two-photon imaging study. *J. Biol. Chem.* **284**, 36109–36117.

LoGuidice, A., and Boelsterli, U. A. (2011). Acetaminophen overdose-induced liver injury in mice is mediated by peroxynitrite independently of the cyclophilin D-regulated permeability transition. *Hepatology* **54**, 969–978.

Masubuchi, Y., Suda, C., and Horie, T. (2005). Involvement of mitochondrial permeability transition in acetaminophen-induced liver injury in mice. *J. Hepatol.* **42**, 110–116.

McGill, M. R., Sharpe, M. R., Williams, C. D., Taha, M., Curry, S. C., and Jaeschke, H. (2012a). The mechanism underlying acetaminophen-induced hepatotoxicity in humans and mice involves mitochondrial damage and nuclear DNA fragmentation. *J. Clin. Invest* **122**, 1574–1583.

McGill, M. R., Williams, C. D., Xie, Y., Ramachandran, A., and Jaeschke, H. (2012b). Acetaminophen-induced liver injury in rats and mice: comparison of protein adducts, mitochondrial dysfunction, and oxidative stress in the mechanism of toxicity. *Toxicol. Appl. Pharmacol.* **264**, 387–394.

Ni, H. M., Bockus, A., Boggess, N., Jaeschke, H., and Ding, W. X. (2012). Activation of autophagy protects against acetaminophen-induced hepatotoxicity. *Hepatology* **55**, 222–232.

Nieminen, A. L., Gores, G. J., Dawson, T. L., Herman, B., and Lemasters, J. J. (1990). Toxic injury from mercuric chloride in rat hepatocytes. *J. Biol. Chem.* **265**, 2399–2408.

Park, Y., Smith, R. D., Combs, A. B., and Kehrer, J. P. (1988). Prevention of acetaminophen-induced hepatotoxicity by dimethyl sulfoxide. *Toxicology* **52**, 165–175.

Pessayre, D., Fromenty, B., Berson, A., Robin, M. A., Letteron, P., Moreau, R., and Mansouri, A. (2012). Central role of mitochondria in drug-induced liver injury. *Drug Metab. Rev.* **44**, 34–87.

Ramachandran, A., Lebofsky, M., Baines, C. P., Lemasters, J. J., and Jaeschke, H. (2011). Cyclophilin D deficiency protects against acetaminophen-induced oxidant stress and liver injury. *Free Radic. Res.* **45**, 156–164.

Ramachandran, R., and Kakar, S. (2009). Histological patterns in drug-induced liver disease. *J. Clin. Pathol.* **62**, 481–492.

Rehman, H., Ramshesh, V. K., Theruvath, T. P., Kim, I., Currin, R. T., Giri, S., Lemasters, J. J., and Zhong, Z. (2008). NIM811 (N-methyl-4-isoleucine cyclosporine), a mitochondrial permeability transition inhibitor, attenuates cholestatic liver injury but not fibrosis in mice. *J. Pharmacol. Exp. Ther.* **327**, 699–706.

Reid, A. B., Kurten, R. C., McCullough, S. S., Brock, R. W., and Hinson, J. A. (2005). Mechanisms of acetaminophen-induced hepatotoxicity: role of oxidative stress and mitochondrial permeability transition in freshly isolated mouse hepatocytes. *J. Pharmacol. Exp. Ther.* **312**, 509–516.

Riordan, S. M., and Williams, R. (2002). Alcohol exposure and paracetamol-induced hepatotoxicity. *Addict. Biol.* **7**, 191–206.

Saito, C., Lemasters, J. J., and Jaeschke, H. (2010a). c-Jun N-terminal kinase modulates oxidant stress and peroxynitrite formation independent of inducible nitric oxide synthase in acetaminophen hepatotoxicity. *Toxicol. Appl. Pharmacol.* **246**, 8–17.

Saito, C., Zwingmann, C., and Jaeschke, H. (2010b). Novel mechanisms of protection against acetaminophen hepatotoxicity in mice by glutathione and N-acetylcysteine. *Hepatology* **51**, 246–254.

Schilling, A., Corey, R., Leonard, M., and Eghtesad, B. (2010). Acetaminophen: old drug, new warnings. *Cleve. Clin. J. Med.* **77**, 19–27.

Shi, Y., Rehman, H., Ramshesh, V. K., Schwartz, J., Liu, Q., Krishnasamy, Y., Zhang, X., Lemasters, J. J., Smith, C. D., and Zhong, Z. (2012). Sphingosine kinase-2 inhibition improves mitochondrial function and survival after hepatic ischemia-reperfusion. *J. Hepatol.* **56**, 137–145.

Theruvath, T. P., Zhong, Z., Pediaditakis, P., Ramshesh, V. K., Currin, R. T., Tikunov, A., Holmuhamedov, E., and Lemasters, J. J. (2008). Minocycline and N-methyl-4-isoleucine cyclosporin (NIM811) mitigate storage/reperfusion injury after rat liver transplantation through suppression of the mitochondrial permeability transition. *Hepatology* **47**, 236–246.

Tirmenstein, M. A., and Nelson, S. D. (1989). Subcellular binding and effects on calcium homeostasis produced by acetaminophen and a nonhepatotoxic regioisomer, 3'-hydroxyacetanilide, in mouse liver. *J. Biol. Chem.* **264**, 9814–9819.

Waldmeier, P. C., Feldtrauer, J. J., Qian, T., and Lemasters, J. J. (2002). Inhibition of the mitochondrial permeability transition by the nonimmunosuppressive cyclosporin derivative NIM811. *Mol. Pharmacol.* **62**, 22–29.

Watkins, P. B., Kaplowitz, N., Slattery, J. T., Colonese, C. R., Colucci, S. V., Stewart, P. W., and Harris, S. C. (2006). Aminotransferase elevations in healthy adults receiving 4 grams of acetaminophen daily: a randomized controlled trial. *JAMA* **296**, 87–93.

Yoon, M. Y., Kim, S. J., Lee, B. H., Chung, J. H., and Kim, Y. C. (2006). Effects of dimethylsulfoxide on metabolism and toxicity of acetaminophen in mice. *Biol. Pharm. Bull.* **29**, 1618–1624.

Youle, R. J., and Narendra, D. P. (2011). Mechanisms of mitophagy. *Nat. Rev. Mol. Cell Biol.* **12**, 9–14.

Zhong, Z., Ramshesh, V. K., Rehman, H., Currin, R. T., Sridharan, V., Theruvath, T. P., Kim, I., Wright, G. L., and Lemasters, J. J. (2008). Activation of the oxygen-sensing signal cascade prevents mitochondrial injury after mouse liver ischemia-reperfusion. *Am. J. Physiol Gastrointest. Liver Physiol.* **295**, G823–G832.

Zhong, Z., Ramshesh, V. K., Rehman, H., Liu, Q., Theruvath, T. P., Krishnasamy, Y., and Lemasters, J. J. (2014). Acute ethanol causes hepatic mitochondrial depolarization in mice: role of ethanol metabolism. *PLoS. One* **9**, e91308.

Zhong, Z., Theruvath, T. P., Currin, R. T., Waldmeier, P. C., and Lemasters, J. J. (2007). NIM811, a mitochondrial permeability transition inhibitor, prevents mitochondrial depolarization in small-for-size rat liver grafts. *Am. J. Transplant.* **7**, 1103–1111.

Zimmerman, H. J., and Maddrey, W. C. (1995). Acetaminophen (paracetamol) hepatotoxicity with regular intake of alcohol: analysis of instances of therapeutic misadventure. *Hepatology* **22**, 767–773.

Zoratti, M., and Szabo, I. (1995). The mitochondrial permeability transition. *Biochim. Biophys. Acta* **1241**, 139–176.